

Measurement of bi-directional ammonia fluxes over soybean using the modified Bowen-ratio technique

J.T. Walker^{a,*}, W.P. Robarge^b, Y. Wu^c, T.P. Meyers^d

^aNational Risk Management Research Laboratory, U.S. Environmental Protection Agency, Research Triangle Park, NC 27711, United States

^bDepartment of Soil Science, North Carolina State University, Raleigh, NC 27695, United States

^cGoddard Space Flight Center, National Aeronautics and Space Administration, Greenbelt, MD 20771, United States

^dAtmospheric Turbulence and Diffusion Division, National Oceanic and Atmospheric Administration, Oak Ridge, TN 37830, United States

Received 23 September 2005; accepted 7 March 2006

Abstract

Measurements of bi-directional ammonia (NH₃) exchange over a fertilized soybean canopy are presented for an 8-week period during the summer of 2002. The modified Bowen-ratio approach was used to determine fluxes from vertical NH₃ and temperature gradients in combination with eddy covariance sensible heat fluxes. The measurement site is located in an area of high NH₃ emissions from animal production and fertilizer use. Ambient NH₃ concentrations ranged from 0.01 to 43.9 μg m⁻³ ($\mu = 9.4 \mu\text{g m}^{-3}$) during the experiment. The mean flux was $-12.3 \text{ ng m}^{-2} \text{ s}^{-1}$, indicating that the canopy was a net sink for NH₃; however, emission fluxes were consistently observed during the late morning and early afternoon. Deposition rates were highest when the canopy was wet ($\mu = -29.9 \text{ ng m}^{-2} \text{ s}^{-1}$). Modeling results suggest that uptake via the leaf cuticle was the dominant deposition process and stomatal uptake only occurred during the first few hours after sunrise when the stomatal resistance and compensation point were low. The average stomatal compensation point was high ($\chi_s = 11.5 \mu\text{g NH}_3 \text{ m}^{-3}$), primarily due to high daytime temperatures ($\mu = 29 \text{ }^\circ\text{C}$). Measured cuticular resistances were large (median $R_w = 208 \text{ s m}^{-1}$), most likely due to very dry conditions. The average NH₃ flux corresponds to a dry-to-wet deposition ratio of 0.44. Median flux error was 51%, which was dominated by uncertainty in the vertical NH₃ gradient due to sequential sampling between measurement heights.

© 2006 Elsevier B.V. All rights reserved.

Keywords: Ammonia; Dry deposition; Compensation point; Soybean; Bi-directional flux

1. Introduction

Ammonia (NH₃) is the most abundant alkaline gas in the atmosphere, and thus plays an important role in the neutralization of acidic gases and aerosols and in the global biogeochemical cycling of nitrogen. Ammonia and ammonium aerosol (NH₄⁺) contribute a significant fraction of atmospheric nitrogen deposition to terrestrial and aquatic ecosystems. Nitrogen input in excess of system requirements can induce environmental stresses

such as soil acidification (Roelofs et al., 1985), forest decline (Nihlgard, 1985), and eutrophication of surface waters (Paerl, 1995; Paerl and Whitall, 1999). For this reason, much work has been done to establish critical loads for nitrogen deposition, which are used in Europe to quantify the sensitivity of ecosystems to nutrient over-enrichment and guide regulatory policy related to nitrogen emissions (see Erisman et al., 2003).

Ammonia is also a precursor to inorganic aerosol compounds, including ammonium sulfate, ammonium bisulfate, ammonium nitrate, and ammonium chloride, which cumulatively account for 40–65% of PM_{2.5} mass in the eastern U.S. (Malm et al., 1994; U.S. EPA, 1996;

* Corresponding author. Tel.: +1 919 541 2288.

E-mail address: walker.johnt@epa.gov (J.T. Walker).

Tolocka et al., 2001). This relationship with $\text{PM}_{2.5}$ currently defines the regulatory importance of NH_3 in the U.S., which has set ambient particulate matter standards in an effort to reduce human health risks associated with inhalation of small particles (U.S. EPA, 1996, 1997). Animal manure, synthetic fertilizer and agricultural crops are the primary sources of atmospheric NH_3 and cumulatively contribute $\approx 64\%$ of global emissions ($53.8 \text{ Tg N year}^{-1}$, $1 \text{ Tg} = 10^{12} \text{ g}$, Bouwman et al., 1997). Subsequently, mixed (i.e., animal and crop production) agricultural regions may experience high concentrations of NH_3 in air and precipitation, along with elevated inorganic $\text{PM}_{2.5}$ concentrations (Walker et al., 2000a, 2004).

Evaluation of atmospheric nitrogen deposition and inorganic aerosol budgets at regional and larger scales requires the use of complex three-dimensional air quality models (Dentener and Crutzen, 1994; Adams et al., 1999; Mathur and Dennis, 2003). These models must accurately depict emissions, transport, atmospheric chemistry, and deposition of nitrogen compounds. In a recent modeling exercise for the eastern U.S., Mathur and Dennis (2003) point out that, while recent improvements have been made to NH_3 emission inventories, major uncertainty still exists regarding the accurate determination of NH_3 air-surface exchange rates. Uncertainty in estimates of uptake or emission from vegetation and soil translates to uncertainty in ecosystem nitrogen budgets and inaccurate prediction of atmospheric NH_3 concentrations. This uncertainty may be particularly important in agricultural regions where the spatial variability of emissions, and therefore deposition, is high.

Measurements of bi-directional NH_3 air-surface exchange at North American sites are limited (Harper et al., 1987; Harper and Sharpe, 1995; Langford et al., 1992; Pryor et al., 2001; Rattray and Sievering, 2001; Phillips et al., 2004). Furthermore, NH_3 flux models developed from more extensive European datasets (Sutton et al., 1998; Nemitz et al., 2000a, 2001) may not be generally applicable to North America due to differences in meteorology, atmospheric chemistry, and vegetation characteristics. European experiments show that dry deposition is high near sources (Fowler et al., 1998), where NH_3 represents the primary ecosystem nitrogen input, and that fluxes are bi-directional further downwind, owing to the presence of a compensation point (Farquhar et al., 1980; Sutton et al., 1995). Measurements over fertilized crops show soil and plant emissions immediately after fertilization and bi-directional exchange with vegetation throughout most of the growing season (Harper et al., 1987;

Harper and Sharpe, 1995; Sutton et al., 1993a). Thus, vegetation can represent both a source and a sink for NH_3 , depending on the atmospheric concentration, meteorology, and surface characteristics. The goal of this project was to measure the air-surface exchange of NH_3 over soybean at a site characterized by elevated atmospheric NH_3 . We present data collected semi-continuously during the middle of the growing season from 6/17/02 (DOY 168) to 8/22/02 (DOY 234).

2. Methods

2.1. Ammonia fluxes

Bi-directional NH_3 air-surface exchange was measured using the modified Bowen-ratio (MBR) technique (Hicks and Wesely, 1978; Duyzer et al., 1992; Meyers et al., 1996). The flux (F_{NH_3}) was calculated as:

$$F_{\text{NH}_3} = \overline{w'T'} \frac{\Delta\text{NH}_3}{\Delta T} = K_H \Delta\text{NH}_3 \quad (1)$$

where $\overline{w'T'}$ is the kinematic sensible heat flux measured by eddy covariance, ΔNH_3 the difference in NH_3 concentration between two heights, and ΔT is the difference in temperature measured over the same vertical distance and time interval as NH_3 . The MBR technique has advantages over the traditional aerodynamic approach in that the eddy diffusivity for sensible heat (K_H) is determined directly and the NH_3 gradient can be determined from measurements at only two heights (Duyzer et al., 1992).

During this experiment, NH_3 fluxes were calculated from 30 min average NH_3 and temperature gradients between $z = 1$ and 5.3 m and eddy covariance sensible heat fluxes measured at $z = 3.2 \text{ m}$. Sensible heat fluxes and three-dimensional wind speeds were measured with a Gill Windmaster Pro sonic anemometer (Gill Instruments Limited, Lymington, Hampshire, United Kingdom). Temperature gradients were measured with precision thermocouples (Omega Engineering Inc., Stamford, CT). Ammonia concentrations were determined by chemiluminescence as discussed below.

2.2. Resistance analogy and compensation point

The air-surface exchange of trace gases has commonly been defined using the resistance analogy, which describes the net flux (F_t) as:

$$F_t = - \frac{\chi_a(z-d) - \chi_0}{R_t(z-d)} \quad (2)$$

where χ_a is the atmospheric concentration at reference height ($z - d$), z the measurement height, d the zero-plane displacement, χ_0 the surface concentration, and R_t is the total resistance to transfer between reference height ($z - d$) and the surface. R_t includes the aerodynamic resistance $R_a(z - d)$, which is governed by turbulent transport, and the boundary layer resistance (R_b), which describes transfer across the sub-laminar boundary layer of the receptor surface. In this case, $R_a(z - d)$ and R_b were estimated from meteorological parameters using the formulations of Garland (1977) and Hicks et al. (1987), respectively.

When the surface concentration χ_0 is zero, Eq. (2) reduces to:

$$F_t = -\frac{\chi_a(z - d)}{R_t(z - d)} = -V_d(z - d)\chi_a(z - d) \quad (3)$$

where $V_d(z - d)$ is the deposition velocity. In this case, the difference between $R_t(z - d)$ and $[R_a(z - d) + R_b]$ may be interpreted as an additional resistance to deposition established by the surface itself, referred to as the canopy resistance (R_c). In the case of NH_3 , deposition to vegetation occurs via exchange through the leaf stomata and uptake by moisture on the leaf cuticle (Sutton and Fowler, 1993). Thus, R_c can be calculated from the stomatal (R_s) and cuticular (R_w) resistances according to (Erisman et al., 1994):

$$R_c = (R_s^{-1} + R_w^{-1})^{-1} \quad (4)$$

In this analysis, R_s was estimated from measured water vapor fluxes according to Monteith and Unsworth (1990), adjusted for the diffusivity of NH_3 .

The R_c approach has been widely applied for inferential modeling of SO_2 , HNO_3 , and O_3 deposition (e.g., Fowler and Unsworth, 1979; Hicks et al., 1987; Wesely, 1989; Meyers et al., 1998). Though the R_c approach has also been used to interpret and model NH_3 fluxes (e.g., Duyzer et al., 1992; Sutton et al., 1993b; Erisman and Wyers, 1993), it clearly does not describe bi-directional exchange. In the case of NH_3 , leaves may act as a source or sink depending on the ratio of the ambient concentration to the stomatal compensation point (χ_s), which is established by the apoplastic concentrations of NH_4^+ and H^+ (Farquhar et al., 1980; Husted and Schjoerring, 1995). When $\chi_0 > 0$, both R_c and $V_d(z - d)$ become dependent on concentration and the concept of deposition velocity is no longer applicable. Sutton et al. (1998) present an alternative to the R_c model in which the competing processes of emission and deposition are taken into account by relating the flux to the net emission potential of the

canopy, or “canopy compensation point” (χ_c), calculated as (Sutton et al., 1993b):

$$\chi_c = \chi_a(z - d) + F_t[R_a(z - d) + R_b] \quad (5)$$

If the net exchange is due to stomatal (F_s) and cuticular (F_w) fluxes only, then the measured flux (F_t) may be expressed as:

$$F_t = F_w + F_s \quad (6)$$

where

$$F_s = \frac{(\chi_s - \chi_c)}{R_s} \quad (7a)$$

and

$$F_w = \frac{-\chi_c}{R_w} \quad (7b)$$

Using Eqs. (5)–(7), Sutton et al. (1998) derived the following relationship for χ_c :

$$\chi_c = \frac{\chi_a(z - d)[R_a(z - d) + R_b]^{-1} + \chi_s R_s^{-1}}{[R_a(z - d) + R_b]^{-1} + R_w^{-1} + R_s^{-1}} \quad (8)$$

Once χ_c is determined, the component fluxes (F_s and F_w) can then be calculated. It should be noted that while the canopy compensation point in Eq. (8) describes the equilibrium surface concentration established by competing source/sink processes, the true compensation point is defined by Eq. (5) as the ambient concentration when $F_t = 0$.

Emissions from the soil and decomposing leaf litter, though often recaptured by the overlying canopy (Meixner et al., 1996; Nemitz et al., 2000b), may at times contribute to the net exchange, especially in sparse or dry canopies. This additional source may be accounted for by adding a soil flux term (F_g) to Eq. (8) (Sutton et al., 1998). However, as pointed out by Sutton et al. (1998), this single-layer approach assumes that exchange takes place at one point in the canopy and is therefore a simplified representation of soil emissions. Though not considered in this analysis, Nemitz et al. (2000a, 2001) present extensions of the single-layer χ_c model to explicitly treat multiple layers (i.e., soil, leaf litter, and canopy components). Though mechanistically less descriptive than the multi-layer models, the single-layer χ_c model provides a suitable framework for interpretation of our fluxes. In this paper we discuss our results within the context of both the R_c and χ_c approaches.

2.3. Ammonia concentration gradients

Ammonia concentrations were measured with a chemiluminescence NO_x/NH_3 analyzer (Model 17C, Thermo Electron Corporation, Franklin, MA). The concentration of NH_3 in air was calculated as the difference between the total nitrogen ($N_T = \text{NO} + \text{NO}_2 + \text{NH}_3$) and NO_x ($\text{NO} + \text{NO}_2$) channels of the instrument, where NO and NO_2 represent nitric oxide and nitrogen dioxide, respectively. To measure N_T , the sample is passed through an external thermal converter (825°C) which converts $\text{NO}_2 + \text{NH}_3$ to NO . The NO from these sources is then detected in the reaction chamber, representing the concentration of N_T . Similarly, NO_x is converted to NO as it passes through an internal molybdenum converter (325°C). The NH_3 concentration is then determined as $N_T - \text{NO}_x$. An external pump draws air through the analyzer at a constant rate of approximately 0.40 L min^{-1} . Switching between the NO_x , N_T , and NO channels is controlled via timed solenoid valves. Instrument zero and span (40.0 ppb) points were checked approximately every 48 h and multipoint calibrations were performed every 2 weeks. Efficiency of the NH_3 converter was periodically checked using a diluted NH_3 standard (10.0 ppm, Scott Specialty Gases, Plumsteadville, PA). The efficiency of the molybdenum NO_x converter was tested by introducing a known concentration of NO_2 . Concentrations were recorded as 1 min averages.

To eliminate the potential sampling error inherent in using two analyzers to determine the NH_3 gradient, a single analyzer was automatically switched between the upper and lower inlets every 15 min. After switching, the NH_3 concentration was allowed to equilibrate for 5 min. The last 10 min of each 15 min period were then used to calculate the gradient. Using this approach, a gradient was determined for each 30 min period and fluxes were analyzed in terms of 30 min values. To minimize NH_3 adsorption on tubing walls, sample air was pulled through heated (50°C) Teflon sample lines at 8 Lpm to the base of the tower where a portion of the sample was drawn into the high temperature NH_3 converter. After conversion of NH_3 to NO , the sample was drawn at 0.40 Lpm to the chemiluminescence analyzer housed in a temperature controlled mobile laboratory. Sample travel distance and time from the inlet to the NH_3 converter were $\approx 7 \text{ m}$ and 2 s, respectively. Travel distance and time from the NH_3 converter to the analyzer were $\approx 23 \text{ m}$ and 90 s, respectively. Loss of NO during transit from the NH_3 converter to the analyzer was assumed to have a negligible effect on the measured gradient.

It is important to note that our NH_3 measurement may have been influenced by the presence of NH_4^+ aerosol. First, some NH_3 may have been produced from NH_4NO_3 volatilization in the heated sample line. Second, the high temperature NH_3 converter also converts an unknown fraction of NH_4^+ aerosol, as well as gas-phase amines. While amine concentrations are expected to be very low, detection of aerosols may, at times, impart a positive bias to the measured NH_3 concentration. As a result of this interference, the measured NH_3 gradient will be influenced by the aerosol gradient. This potential source of error in the measured NH_3 flux is addressed in the following analysis.

2.4. Ancillary measurements

In addition to NH_3 and sensible heat fluxes, the remaining components of the surface energy balance were measured along with standard meteorological parameters. Single-sided leaf area index (LAI) was measured approximately bi-weekly (Model LAI2000 Plant Canopy Analyzer, LI-COR Inc., Lincoln, NE) at random locations along 150 m transects to the east and west of the sampling tower. Soil samples were taken approximately bi-weekly at 0–10, 10–20, and 20–30 cm depths at random locations within $2 \text{ m} \times 2 \text{ m}$ subplots inside a $100 \text{ m} \times 100 \text{ m}$ sampling grid. Samples were analyzed for soil available NO_3^- and NH_4^+ using standard 2 M KCl extraction and colorimetric analysis (Model 8000 Flow Injection Analyzer, Lachat Instruments, Milwaukee, WI). Above-ground biomass (leaf and stalk) was collected approximately bi-weekly from $1 \text{ m} \times 1 \text{ m}$ plots randomly selected along 150 m transects to the east and west of the sampling tower and analyzed for total nitrogen and carbon (Model 2400 Elemental Analyzer, Perkin-Elmer, Boston, MA). Soil volumetric water was measured continuously at a depth of 10 cm (Model CS616 Water Content Reflectometer, Campbell Scientific Inc., Logan, UT).

3. Site characteristics

3.1. Location

The study site was located in Duplin County, North Carolina, in the state's Upper Coastal Plain physiographic region. This area of the state is characterized by high NH_3 emissions from animal production and fertilizer use (Walker et al., 2000b). There are numerous animal production facilities, primarily swine and turkey, within the general vicinity of the study site and the nearest facility is approximately 1.5 km to the northeast. The

annual mean NH_3 concentration in this area is $\approx 5.50 \mu\text{g m}^{-3}$ and NH_3 accounts for $>70\%$ of total $\text{NH}_3 + \text{NH}_4^+$ (Robarge et al., 2002). As a result of the temperature dependence of NH_3 emissions from animal manure and fertilized soil (Aneja et al., 2000), concentrations of NH_3 and NH_4^+ in air and precipitation (Robarge et al., 2002; Walker et al., 2000b) are highest at this site during the summer.

The study site was a 90 ha agricultural field bordered by mature pine trees to the north, east, and south and additional agricultural fields to the west and southwest. The sampling tower was positioned such that the perimeter of the field established fetch lengths of 210, 300, 350, and 375 m to the north, east, south, and west, respectively. This position was chosen to achieve a maximum fetch extending toward the southwest (600 m), which is the predominant wind direction at this site during the summer. The soybean [*Glycine max* (L.) Merr.] crop was planted on 5/20/02 and the field was fertilized with poultry litter at a rate of $\approx 65 \text{ kg N ha}^{-1}$ 2 weeks prior to planting. Soil at the site is Norfolk series fine sandy loam (USDA, 1954).

4. Results and discussion

4.1. Soil and plant conditions

Average soil NO_3^- and NH_4^+ concentrations (0–10 cm depth) were 3.93 and 1.38 mg N kg (dry soil) $^{-1}$, respectively. Nitrate concentrations showed a slight increase throughout the experiment, which was likely due to nitrification of NH_4^+ in the poultry litter applied prior to the experiment. Soil NH_4^+ concentrations showed high spatial variability which precluded the detection of temporal trends. Soybean biomass (leaf and stalk) was 42.5% carbon and 3.0% nitrogen, on average, though nitrogen content declined during the course of the experiment coincident with increasing carbon. Fig. 1 shows single-sided leaf area index (LAI) and hourly soil volumetric water at 10 cm depth during the experiment. As indicated by the spikes in soil volumetric water ($\text{m}^3 \text{ m}^{-3}$), rainfall occurred infrequently. Events on DOY 177–178 (10.4 cm) and DOY 191–192 (10.3 cm) contributed 51% of total rainfall (40.4 cm) during the experiment. Soil volumetric water at 10 cm depth averaged 7.3%, which is near the permanent wilting point for sandy loam soils (Brady and Weil, 1999). The soybean canopy often showed visible signs of drought stress, particularly during late afternoon. LAI reached a maximum of $4.4 \text{ m}^2 \text{ m}^{-2}$ near DOY 200 before the onset of insect damage, which reduced LAI to $\approx 2.2 \text{ m}^2 \text{ m}^{-2}$ by the end of the experiment.

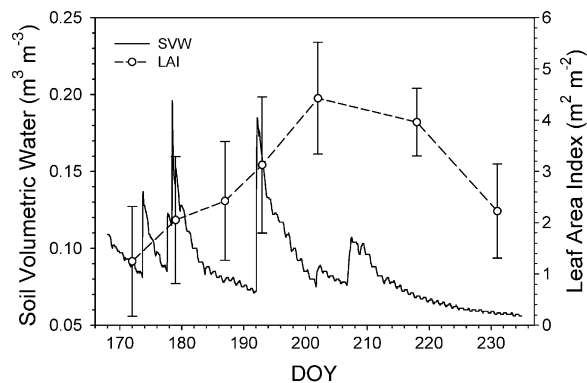


Fig. 1. Soil volumetric water (SVW) at 10 cm (solid line) and single-sided leaf area index (LAI) (circles) during the course of the experiment. Values of soil volumetric water represent hourly averages. Leaf area index represents the average value from six locations. Error bars represent ± 1 standard deviation of the mean.

4.2. Ammonia concentrations and fluxes

Ammonia concentrations ranged from 0.01 to $43.9 \mu\text{g m}^{-3}$ during the experiment, and mean and median values were 9.4 and $8.6 \mu\text{g m}^{-3}$ ($N = 1599$), respectively. These values are similar to those reported by Robarge et al. (2002) and Walker et al. (2004) at a nearby site during previous years. Fig. 2 shows the

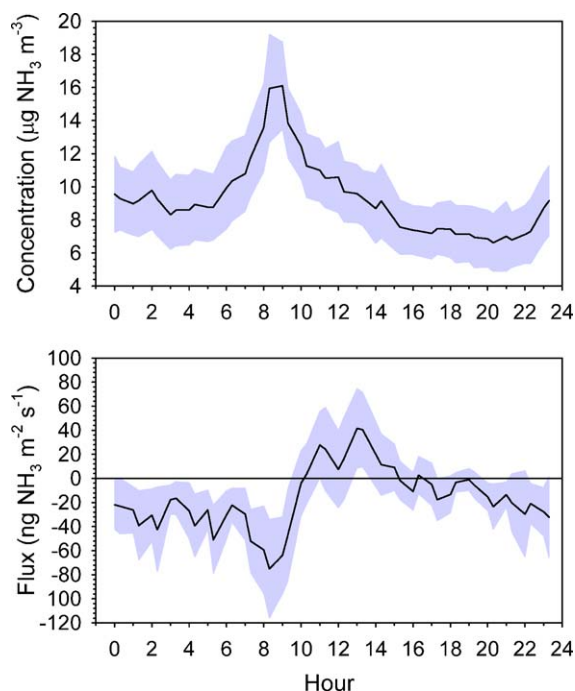


Fig. 2. Average diurnal profiles of NH_3 concentration ($z - d = 2.6 \text{ m}$) and flux. Data represent average values for individual 30 min periods. Gray area represents the 95% confidence interval of the mean for each 30 min period. Negative fluxes indicate deposition.

average diurnal concentration profile which peaked in the morning and reached a minimum near sunset. On most nights, the concentration began to gradually increase between 1 and 4 a.m. followed by a period of more rapid increase beginning just after sunrise. The initial increase was likely the result of NH_3 accumulation within the shallow nocturnal boundary layer. The period of rapid increase after sunrise may have been caused by downward mixing of NH_3 from above the surface layer or venting from local ground-level sources. Concentrations began to decrease between 8 and 10 a.m. as the daytime mixed layer developed. In general, NH_3 concentrations were highest when winds were from the southwest, which is the upwind direction of a relatively dense population of animal production facilities.

Prior to analysis, fluxes were filtered to exclude low wind speeds ($\bar{u} < 0.5 \text{ m s}^{-1}$), and periods when fetch requirements were not met. Using the footprint model of Hsieh et al. (2000), fluxes were rejected if the soybean field contributed $< 80\%$ of the flux at the midpoint of the NH_3 concentration gradient ($z = 3.2 \text{ m}$). Filtering by these criteria reduced the number of 30 min flux values from 1599 to 1113. The final flux dataset is summarized in Table 1. The mean flux including all data points was $-12.3 \text{ ng m}^{-2} \text{ s}^{-1}$, indicating that the soybean canopy was a net sink for NH_3 during the study period. On average, the flux was more strongly negative (i.e., deposition) at night (Table 1), though the highest deposition fluxes typically occurred after sunrise (Fig. 2), coincident with the diurnal peak in NH_3 concentrations. Deposition rates were significantly higher when the canopy was wet ($\mu = -29.9 \text{ ng m}^{-2} \text{ s}^{-1}$, $N = 196$). Emission fluxes occurred most frequently during the day when the canopy was dry, and were rarely observed during wet periods (Table 1). As shown in Fig. 2, emissions were observed during the late morning and early afternoon coincident with decreasing atmospheric NH_3 concentrations and increasing temperature.

The average NH_3 flux corresponds to a deposition rate of $0.81 \text{ kg NH}_3\text{-N ha}^{-1}$ during the period 6/1/02–9/1/02. For comparison, wet deposition of $\text{NH}_4^+\text{-N}$ measured at nearby National Atmospheric Deposition Program site NC35 was approximately 1.85 kg ha^{-1} (NADP, 2004) during the same period, which corresponds to a dry-to-wet deposition ratio of 0.44. The ratio of NH_3 dry deposition to total inorganic nitrogen wet deposition ($\text{NH}_4^+ + \text{NO}_3^-$) was 0.27. The primary nitrogen inputs to the soybean system were from fertilization (65 kg N ha^{-1}) and nitrogen fixation, which averaged approximately 150 kg N ha^{-1} at 100

Table 1
Summary of fluxes ($\text{ng m}^{-2} \text{ s}^{-1}$) during periods of emission only, deposition only, and for the entire dataset (emission + deposition)

	Mean	Median	S.D.	Max.	Min.	N
Emission						
Dry						
Day	42.1	29.0	46.9	326.5	0.0	360
Night	6.8	3.5	7.7	28.1	0.0	38
Wet						
Day	33.4	22.8	29.5	106.6	0.4	35
Night	11.3	8.9	10.4	38.3	1.4	13
All emission	37.5	23.3	44.4	326.5	0.0	446
Deposition						
Dry						
Day	-48.6	-28.2	60.2	0.0	-395.1	349
Night	-37.1	-21.7	39.0	0.0	-169.6	170
Wet						
Day	-71.1	-49.2	90.3	-0.7	-447.5	65
Night	-30.8	-18.0	40.0	-0.4	-172.6	83
All deposition	-45.7	-25.7	58.1	0.0	-447.5	667
Emission + deposition						
Dry						
Day	-2.5	0.2	70.4	326.5	-395.1	709
Night	-29.1	-16.3	39.3	28.1	-169.6	208
Wet						
Day	-34.5	-8.7	89.9	106.6	-447.5	100
Night	-25.1	-9.7	40.1	38.3	-172.6	96
All emission + deposition	-12.3	-4.1	66.9	326.5	-447.5	1113

Daytime is defined as $\text{PAR} > 50 \mu\text{mol m}^{-2} \text{ s}^{-1}$ and wetness is determined by the leaf wetness sensor. Negative fluxes indicate deposition.

days after planting in a variety of cultivars grown at a nearby site (Israel and Burton, 1997). The total input of reduced nitrogen ($\text{NH}_3 + \text{NH}_4^+$) from the atmosphere was equivalent to 1.9% of the nitrogen fixed by the plants and 4.2% of fertilizer nitrogen. Israel and Burton (1997) found that nitrogen fixation supplied between 65 and 75% of the crop requirement when grown on sandy soils typical of eastern North Carolina. We may therefore conclude that dry and dry + wet deposition of NH_3 contributed 0.3 and 1.2% of crop nitrogen requirements.

4.3. Compensation points

The flux bi-directionality shown in Fig. 2 is consistent with the presence of a canopy compensation point, which can be estimated by examining the relationship between flux and concentration (Fig. 3). The x -intercept of the solid line fit to the entire dataset is

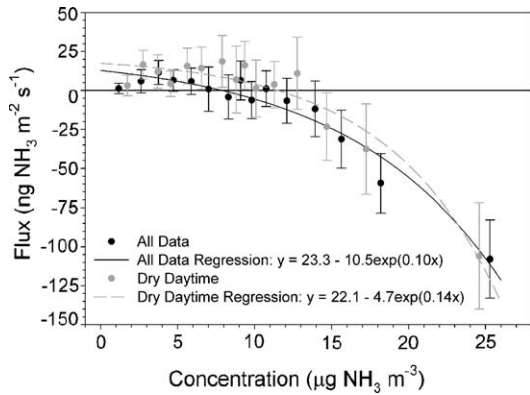


Fig. 3. Relationship between NH_3 flux and concentration ($z - d = 2.6$ m). Black circles represent bin-averaged values for the entire dataset. Gray circles represent bin averages of only those values with $\text{PAR} > 50 \mu\text{mol m}^{-2} \text{s}^{-1}$ and dry conditions as indicated by the leaf wetness sensor. Solid and dashed lines represent best-fit curves for mean values. Error bars represent the 95% confidence interval of the mean. Negative fluxes indicate deposition.

an estimate of χ_c ($7.9 \mu\text{g NH}_3 \text{m}^{-3}$, $N = 1113$). In this case, the equilibrium concentration corresponding to $F_t = 0$ is established by both cuticular (nighttime, wet periods) and stomatal processes (daytime) as well as exchange with the soil and leaf litter. The value of χ_c determined from Fig. 3 is consistent with the median value ($7.4 \mu\text{g m}^{-3}$) calculated from Eq. (5). The dashed curve in Fig. 3 relates flux to concentration during dry (leaf wetness = 0) daytime ($\text{PAR} > 50 \mu\text{mol m}^{-2} \text{s}^{-1}$) periods only, when R_w is expected to be large. Assuming that soil exchange is negligible, the equilibrium concentration at $F_t = 0$ under these conditions represents an estimate of χ_s . In this case, $\chi_s = 11.5 \mu\text{g m}^{-3}$ ($N = 709$) which is on the upper end of the range of stomatal compensation points ($0.7\text{--}15 \mu\text{g m}^{-3}$) previously reported for agricultural systems (Dabney and Bouldin, 1990; Sutton et al., 1993a; Harper et al., 1996; Yamulki et al., 1996; Husted et al., 2000; van Hove et al., 2002). The non-linearity of the curves in Fig. 3 suggests a constant emission flux at low NH_3 concentrations. This may reflect afternoon stomatal emission, since NH_3 concentrations were low and relatively constant between 4 and 8 p.m. (Fig. 2). Possible non-stomatal emission sources include the soil, decaying leaf litter, and volatilization from the leaf cuticle. Volatilization from the leaf cuticle is most likely to occur in the morning as the canopy dries and therefore is an unlikely explanation for the observed emission flux. It is possible that emissions from the soil and decaying plant litter contributed at least partly to the constant flux observed at low NH_3 (Nemitz et al., 2000b; Harper et al., 2000).

The stomatal compensation point (χ_s) is a function of temperature and the apoplastic concentrations of NH_4^+ and H^+ , and can be calculated directly as (Nemitz et al., 2000a):

$$\chi_s = \frac{161,500}{T} \exp\left(-\frac{10,380}{T}\right) \frac{[\text{NH}_4^+]}{[\text{H}^+]} \quad (9)$$

where T is canopy temperature in Kelvin and all concentrations are in mol L^{-1} . The leaf emission potential $\Gamma_s = [\text{NH}_4^+]/[\text{H}^+]$ is an important physiological control over canopy-scale NH_3 fluxes and has been shown to vary widely as a function of plant and soil nitrogen status. For example, Schjoerring et al. (1998) found that Γ_s ranged from 55 to 672 in *Brassica napus* L. leaves of plants receiving low and high nitrogen inputs, respectively. In a study of NH_3 exchange over a high nitrogen agricultural grassland, Sutton et al. (1997) found Γ_s equivalent to 12,620 and 3150 for short and long grasses, respectively. By contrast, estimates of Γ_s derived from measurements at relatively clean Scottish sites over semi-natural vegetation were found to be less than 150 (Flechard and Fowler, 1998; Milford et al., 2001).

One method of estimating Γ_s in Eq. (9) from micrometeorological flux measurements is to examine the relationship between ambient NH_3 concentration and temperature during dry daytime periods when the net canopy flux changes direction (Nemitz et al., 2004). During our experiment, changes in the direction of the flux were often accompanied by relatively rapid changes in ambient concentration, making such an analysis impractical. Instead we have followed an approach similar to Spindler et al. (2001) in which χ_s was derived as in Fig. 3 for a range for temperatures. For this analysis, three curves were generated, corresponding to $T < 28.5$, $28.5 < T < 32.3$, and $T > 32.3$ °C. Categorizing the data in this way yielded $N \approx 235$ observations in each of the three temperature bins. For each curve, χ_s and corresponding mean temperature (T) were then used to estimate Γ_s from Eq. (9). Results (Table 2) show a positive correlation between χ_s and T

Table 2

Stomatal compensation point (χ_s) calculated as the ambient concentration corresponding to zero flux during dry daytime periods

	T_μ (°C)	χ_s ($\mu\text{g m}^{-3}$)	Γ_s
$T < 28.5$	26.5	8.3	1013
$28.5 < T < 32.3$	29.9	12.6	1054
$T > 32.3$	33.3	13.8	798

χ_s is determined for three temperature ranges: $T < 28.5$, $28.5 < T < 32.3$, and $T > 32.3$ °C. The leaf emission potential (Γ_s) is calculated from χ_s and mean temperature (T_μ) using Eq. (9).

Table 3
Summary of deposition velocities ($z - d = 2.6$ m)

	Mean	Median	S.D.	Max.	Min.	N
Dry						
Day	4.3	3.3	4.2	23.7	0.0	349
Night	3.5	2.3	3.8	19.4	0.0	170
Wet						
Day	4.9	3.7	4.9	20.2	0.1	65
Night	5.7	3.2	9.0	60.9	0.0	83
All data	4.3	3.0	5.0	60.9	0.0	667

Deposition velocity is reported in mm s^{-1} . Daytime is defined as $\text{PAR} > 50 \mu\text{mol m}^{-2} \text{s}^{-1}$ and wetness is determined by the leaf wetness sensor. Data represent periods of deposition only.

and the mean value of $\Gamma_s = 955$ is within the range of values reported for systems receiving nitrogen fertilizer. By comparison to European experiments, our results clearly show that the relatively high stomatal compensation points observed in this study were the result of high T rather than high Γ_s .

4.4. Deposition velocity and canopy resistance

Deposition velocities, summarized in Table 3, were calculated from measured fluxes and ambient concentrations during periods of deposition. Having established that the net exchange was partially controlled by a stomatal compensation point, the reported deposition velocities should be interpreted as lower limits. Highest deposition velocities occurred during the day as a result of turbulent mixing acting to minimize the atmospheric resistances. Day and nighttime average deposition velocities were significantly higher when the canopy was wet (Table 3). Fig. 4 shows the average diurnal cycle of $V_d(2.6 \text{ m})$ along with the theoretical maximum

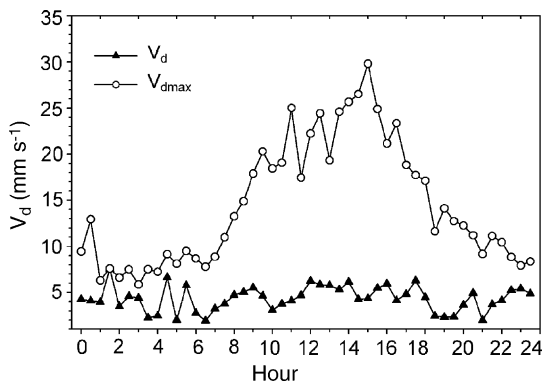


Fig. 4. Average diurnal profiles of $V_d(2.6 \text{ m})$ (triangles) and $V_{dmax}(2.6 \text{ m})$ (circles). Data points represent average values for individual 30 min periods.

Table 4
Summary of aerodynamic (R_a), boundary layer (R_b), and canopy resistances (R_c)

	$R_a(2.6 \text{ m})$	R_b	R_c	N
Dry				
Day	32.6	22.7	214.7	300
Night	80.1	42.5	229.1	147
Wet				
Day	47.8	29.6	146.6	52
Night	73.9	40.2	170.5	51
All data	46.7	28.3	202.4	550

Daytime is defined as $\text{PAR} > 50 \mu\text{mol m}^{-2} \text{s}^{-1}$ and wetness is determined by the leaf wetness sensor. Median values are reported in s m^{-1} .

deposition velocity $V_{dmax}(z - d) = 1/[R_a(z - d) + R_b]$. V_d was less than V_{dmax} at all times, which is consistent with the presence of a significant canopy resistance.

During periods of deposition, the bulk canopy resistance can be calculated as $R_c = 1/V_d(z - d) - 1/V_{dmax}(z - d)$. However, R_c is defined for a perfectly adsorbing surface and should be viewed as an upper limit when $\chi_0 > 0$. Values of R_c are very uncertain when turbulence is low, therefore data were filtered to exclude values of $u_* < 0.05 \text{ m s}^{-1}$. Component resistances are summarized in Table 4. Canopy resistances were largest at night during dry periods and lowest during the day when the canopy was wet. Wetness reduced median day and nighttime R_c values by 32 and 26%, respectively. During dry periods, the median daytime canopy resistance for NH_3 (215 s m^{-1}) was similar to the median stomatal resistance to water vapor transfer (R_s) (193 s m^{-1}).

Assuming NH_3 exchange at the soil surface is negligible, $R_w \approx R_c$ at night when stomata are closed (i.e., $F_t = F_w$). Previous studies (see Nemitz et al., 2001) have shown an exponential decrease in R_w with increasing relative humidity (RH). In the present study, R_w was insensitive to RH below 90%, which suggests that considerable moisture was required on the leaf cuticle before NH_3 uptake could proceed. Furthermore, R_w was large even when the canopy was wet (Table 4). These findings suggest that R_w was affected by the chemical characteristics of the cuticle. Fowler et al. (1998) showed that R_c increased with NH_3 concentration as the cuticle became saturated. Also, Nemitz et al. (2001) summarized data from a number of European field studies which show a negative correlation between R_w and the atmospheric SO_2/NH_3 molar concentration ratio. Neutralization of cuticular water layers by SO_2 increases the NH_3 adsorption capacity (Flechard et al., 1999). The SO_2/NH_3 molar concentration ratio at our

study site is ≈ 0.06 during the summer, which is lower than the values compiled by Nemitz et al. (2001). The infrequency of rainfall during the present study most likely increased the influence of surface chemistry on R_w by allowing NH_3 to accumulate on the cuticle.

In general, observed canopy resistances were somewhat larger than those found in previous studies. For example, Duyzer (1994) and Fowler et al. (1998) report median values of 15–30 and 7–140 s m^{-1} at heathland and moorland sites, respectively. Duyzer et al. (1994) report a median value of 20–25 over a Douglas Fir forest. Similar values were found for corn (Denmead et al., 1978) and alfalfa (Dabney and Bouldin, 1990). Sutton et al. (1993b) report a relatively high mean (125 s m^{-1}) value for calcareous grassland which they suggest may have been explained by the presence of alkaline soil particles on leaf surfaces. While our results indicate that R_w was influenced by the chemical characteristics of the leaf cuticle, it is unknown whether NH_3 saturation or co-deposition (i.e., SO_2) was the more important process. Previously reported canopy resistances suggest that uptake of NH_3 during the day typically occurs at a faster rate than can be explained by stomatal processes alone, which is usually attributed to additional uptake via the leaf cuticle. It is therefore likely that the dry conditions experienced during our study contributed to the high canopy resistances observed during daytime periods. Another explanation for the relatively low observed deposition velocities and high canopy resistances is the potential influence of NH_4^+ aerosol deposition on the measured NH_3 flux. This possibility is discussed in Section 4.6.

4.5. Application of the canopy compensation point model

Data were further analyzed by comparing observed fluxes to those predicted by the single-layer χ_c model (Eq. (8)). Atmospheric and stomatal resistances were calculated as previously described. Since a suitable parameterization for R_w could not be derived, constant values of 229 and 171 s m^{-1} were used for dry and wet periods, respectively (Table 4). Fig. 5 (panel a) shows the average diurnal flux along with three model runs corresponding to different combinations of Γ_s and F_g . Specifying $\Gamma_s = 955$ and $F_g = 0$, the predicted flux compares well with observed deposition fluxes in the afternoon and at night. However, the early morning period of emissions is not predicted. The influence of soil emissions was tested by adding a soil flux term (F_g) to Eq. (8) (Sutton et al., 1998). An upper limit of

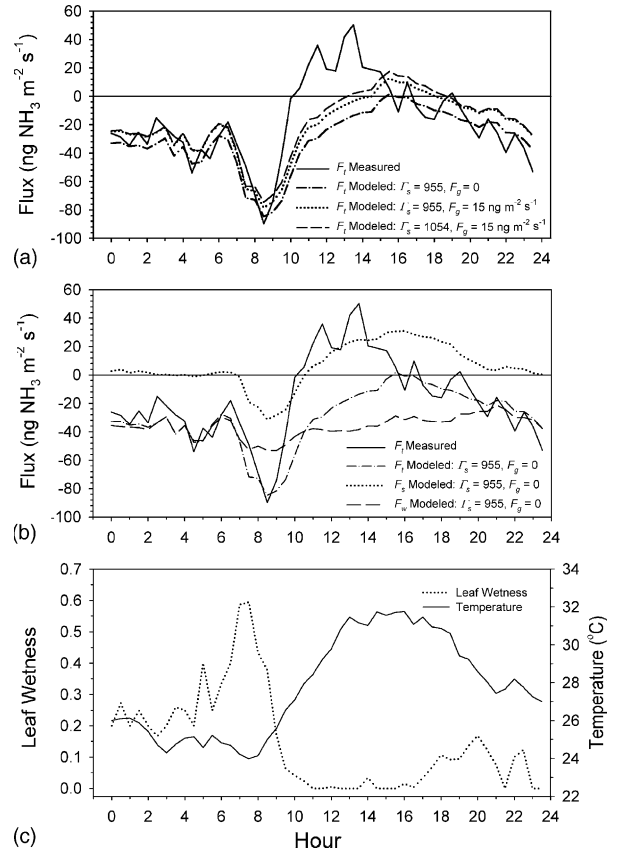


Fig. 5. Comparison of the observed diurnal NH_3 flux with estimates derived from the χ_c model. Panel (a) shows the net flux (F_t) for different combinations of the leaf emission potential (Γ_s) and soil emission (F_g). Panel (b) shows the component fluxes (F_t , F_s and F_g) for $\Gamma_s = 955$ and $F_g = 0$. Panel (c) shows the diurnal cycle of leaf wetness and air temperature. Values of leaf wetness represent the fraction of the 30 min measurement period during which the sensor was wet. Negative fluxes indicate deposition.

$F_g = 15 \text{ ng NH}_3 \text{ m}^{-2} \text{ s}^{-1}$ was chosen by assuming that the positive flux observed at low NH_3 concentrations (Fig. 3) represents emission from the soil only. Specifying $\Gamma_s = 955$ and $F_g = 15 \text{ ng NH}_3 \text{ m}^{-2} \text{ s}^{-1}$ reduces the magnitude of predicted deposition fluxes at night and produces a brief period of emission in the afternoon. Increasing Γ_s to the maximum observed value ($\Gamma_s = 1054$, Table 2) while maintaining $F_g = 15 \text{ ng NH}_3 \text{ m}^{-2} \text{ s}^{-1}$ produces slightly higher emissions.

While the model reproduces nighttime deposition fluxes, the observed period of emission in the morning is not predicted. Furthermore, the emission period is not reproduced by specifying a static soil emission or by increasing Γ_s to the highest observed value. This is expected for constant Γ_s , since the stomatal compensation point is a function of temperature and therefore

reaches a maximum in the late afternoon. The period of morning emission could reflect the presence of a dynamic soil flux (Nemitz et al., 2001), dynamic stomatal compensation point, or emission from the leaf cuticle (Sutton et al., 1998). The diurnal cycle of leaf wetness (Fig. 5, panel c) suggests that the morning emission period is related to drying of the canopy. As the canopy dries, the cuticular resistance would be expected to increase as water layers and droplets evaporate. During the final phase of drying, a period of emission from the cuticle likely occurs. This may partially explain the period of decreasing deposition beginning at 8 a.m., but, since the canopy is typically dry by 10 a.m., does not explain the period of emission during the late morning. However, it is likely that the canopy dries at a slower rate than the surface of the leaf wetness sensor.

Another possibility is that the observed morning period of emission represents a larger stomatal flux than predicted, which would suggest that Γ_s has a diurnal cycle. Fig. 5 (panel b) shows the component modeled fluxes (F_t , F_s , and F_w) for $\Gamma_s = 955$ and $F_g = 0$. There is period of stomatal uptake between 8 and 10 a.m. that follows the pattern of ambient NH_3 concentration. If the rate of NH_3 flux into the apoplast fluid during this period is faster than the rate of NH_4^+ assimilation, then Γ_s would be expected to increase (Mattsson and Schjoering, 2002). This process may be enhanced by uptake of NH_3 emitted from the cuticle as the canopy dries. It is therefore possible that the period of emission observed between 10 and 12 a.m. represents an enhanced stomatal flux due to a diurnal peak in Γ_s .

Though the observed and modeled fluxes disagree during the morning, which may illustrate the dynamic nature of Γ_s and F_w , values of Γ_s and R_w derived from average conditions produce a reasonable representation of the net exchange in the afternoon and at night. Interestingly, stomatal emission during the late afternoon, which is a response to high temperature, must be offset by simultaneous cuticular uptake to reproduce the observed deposition flux. Agreement between observed and modeled F_t suggests that soil emission was not a significant component of the net exchange. This is expected, given the observation of low soil available NH_4^+ and dry conditions.

4.6. Flux uncertainty

Uncertainty in the measured NH_3 flux can result from analytical imprecision and inaccuracy as well as sampling error caused by spatio-temporal variability in atmospheric concentrations, which includes storage errors due to changes in concentration over time,

advection errors due to horizontal concentration gradients, and chemical reactions (Fowler and Duyzer, 1989; Sutton and Fowler, 1992; Flechard and Fowler, 1998). Non-stationarity of the NH_3 concentration in the form of a temporal trend can also produce an artificial gradient when the concentration is intermittently (sequentially) sampled at multiple heights, which was the approach taken during our experiment. In this analysis, error in the calculated NH_3 flux was quantified as the combined error of the variables in Eq. (1) plus the error associated with intermittent sampling of the NH_3 concentration at different heights.

The NH_3 gradient detection limit was determined as a function of analytical precision for NH_3 . Analytical precision was calculated as the relative standard deviation (R.S.D.) of 1 min average NH_3 concentrations over a 15 min period during which a known concentration of NH_3 was sampled (Fig. 6). This test was performed for the range of observed NH_3 concentrations. Using the equation from Fig. 6, precision was then predicted as a function of concentration. The fractional error in the gradient resulting from analytical precision was calculated as $\varepsilon_{P(\Delta\text{NH}_3)} = [(\varepsilon_{\text{NH}_3(H1)})^2 + (\varepsilon_{\text{NH}_3(H2)})^2]^{1/2}$, where $\varepsilon_{\text{NH}_3(H1)}$ and $\varepsilon_{\text{NH}_3(H2)}$ represent the estimated analytical precision at measurement heights 1 and 2, respectively. The gradient detection limit, expressed as a concentration, was then calculated as $\Delta\text{NH}_{3\text{DL}} = (\varepsilon_{\text{NH}_3(H1)} \cdot \mu_{H1} + \varepsilon_{\text{NH}_3(H2)} \cdot \mu_{H2})$, where μ_{H1} and μ_{H2} are the mean concentrations at heights 1 and 2, respectively. Using this approach, 76% of the observed gradients were larger than the predicted gradient detection limit.

Potential error in the measured gradient due to intermittent sampling was tested by placing the upper and lower inlets at the same height, in standard sampling mode, for a period of 5 days. In this configuration, any concentration difference between the two inlets was the result of a temporal trend in

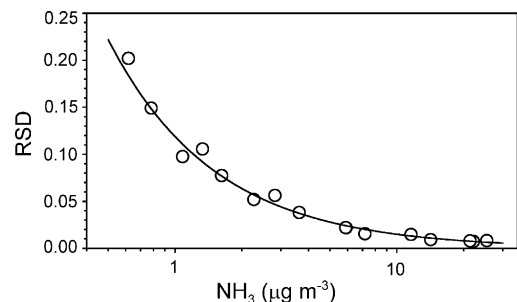


Fig. 6. Analytical precision of the chemiluminescence system, expressed as relative standard deviation (R.S.D.), as a function of NH_3 concentration.

concentration (i.e., artificial gradient), systematic error between the two inlets, analytical precision, and random error. For this analysis, we assumed that the influence of analytical precision was small relative to the influence of intermittent sampling and could therefore be neglected. No systematic error between the two inlets was detected.

The difference in successive 15 min averages at different heights is a result of the real gradient established by deposition or emission processes and the artificial gradient due to intermittent sampling of the NH_3 concentration. The difference in successive 15 min average concentrations at the same height, however, is only a result of intermittent sampling. In this case, the presence of non-stationarity (i.e., trend) in the NH_3 time series was tested by comparing the means of successive same height averages using the Wilcoxon rank sums test, which is the non-parametric analogue of the two-sample t -test. Using this approach, approximately 44% of the gradients measured during the error experiment showed evidence of non-stationarity.

Next, potential error in single 15 min averages due to intermittent sampling was quantified by assessing the difference in single-height (15 min) and corresponding 30 min average concentrations as a function of the difference between previous and following same height averages. For example, the error-induced fractional difference between the 15 min average for height 1 and the corresponding average of heights 1 and 2 over a 30 min period was viewed as a function of the fractional difference between the previous and following 15 min average concentrations for height 1. The resulting linear relationship ($R^2 = 0.57$) was then applied to the flux dataset to predict the error-induced fractional difference between the 15 min single-height average and the 30 min average over which the gradient was calculated. The artificial gradient resulting from intermittent sampling is then the combined fractional error of the mean concentration during the two 15 min periods from which the gradient was calculated. Using this approach, the median error in the calculated gradient due to intermittent sampling ($\varepsilon_{\text{IS}(\Delta\text{NH}_3)}$) was 40% for the entire study.

Error in the kinematic sensible heat flux was determined from duplicate measurements made with identical sonic anemometers separated 2 m horizontally. Fractional error was calculated as the percent difference between the duplicate flux measurements. Systematic error (i.e., accuracy, bias) between the two systems was first assessed using reduced major axis regression (Ayers, 2001), which is appropriate when both regression variables contain error. No systematic

error between the two systems was detected. As illustrated by Thompson and Howarth (1976), random error (i.e., precision) can be determined from paired samples as the median of the relative percent difference between duplicates. Using this approach, the precision of 30 min kinematic sensible heat fluxes ($\varepsilon_{w'T'}$) measured continuously over a period of 5 days ($N = 235$) was 10.9%. These results agree well with Finkelstein and Sims (2001) who found the average fractional error in sensible heat fluxes at three agricultural sites to be $\approx 11.0\%$.

The temperature gradient was determined by continuously measuring the difference in temperature between two heights. Thus, sampling error in the temperature gradient is a function of the accuracy and precision of the thermocouples. In this case, the sensors were placed at the same height and sampling error was assessed by comparing the difference in measured temperatures ($^\circ\text{C}$). Systematic error, calculated in the same way as kinematic heat flux, was found to be 0.04°C ($N = 348$), with the lower thermocouple biased high. Thermocouple precision (ε_T) calculated from duplicate measurements as described above was found to be 0.21%. Precision of the temperature gradient ($\varepsilon_{\Delta T}$) was then calculated as $\varepsilon_{\Delta T} = [(\varepsilon_{T(H1)})^2 + (\varepsilon_{T(H2)})^2]^{1/2} = 0.30\%$, where $\varepsilon_{T(H1)}$ and $\varepsilon_{T(H2)}$ represent the fractional error in the temperature measurement at heights 1 and 2, respectively.

Total error in the measured flux is a function of the combined uncertainty of the variables in Eq. (1). The probable error (δ) of a quantity (y) dependent on $x = 1$ to N independent variables is given by:

$$\delta_y = \left[\left(\frac{\delta_{x_1} \partial y}{\partial x_1} \right)^2 + \left(\frac{\delta_{x_2} \partial y}{\partial x_2} \right)^2 + \dots + \left(\frac{\delta_{x_n} \partial y}{\partial x_n} \right)^2 \right]^{1/2} \quad (10)$$

Probable error in the eddy diffusivity for sensible heat is given by:

$$\delta_{K_H} = \left[\left(\frac{\delta_{w'T'}}{\Delta T} \right)^2 + \left(\frac{(\overline{w'T'}) \delta_{\Delta T}}{(\Delta T)^2} \right)^2 \right]^{1/2} \quad (11)$$

Probable errors in the heat flux (δ_H) and temperature gradient ($\delta_{\Delta T}$), expressed in the appropriate units, were calculated from their respective sampling errors $\varepsilon_{w'T'}$ and $\varepsilon_{\Delta T}$ described above. Probable error in the measured NH_3 flux is then given by:

$$\delta_{F_{\text{NH}_3}} = [(\delta_{K_H} \Delta\text{NH}_3)^2 + (\delta_{\Delta\text{NH}_3} K_H)^2]^{1/2} \quad (12)$$

where probable error in the NH_3 gradient ($\delta_{\Delta\text{NH}_3}$) is determined from the total fractional error due to

analytical precision and intermittent sampling (i.e., $\delta_{\Delta\text{NH}_3} = [(\varepsilon_{\text{IS}(\Delta\text{NH}_3)})^2 + (\varepsilon_{\text{P}(\Delta\text{NH}_3)})^2]^{1/2}$). Using this approach, the median error of the measured flux was 51%, which was dominated by uncertainty due to intermittent sampling. However, given that the majority of the error considered is non-systematic, longer-term averages will be much more robust. For comparison, Flechard and Fowler (1998) estimated mean errors in the range of 30–40% for NH_3 fluxes measured using a three-height aerodynamic method. In that case, flux uncertainty was dominated by random scatter in the vertical concentration profile. The uncertainty calculations for our dataset likely represent an upper limit since the estimate of uncertainty due to intermittent sampling includes some error due to analytical precision, which therefore may have been counted twice in this analysis.

An additional source of error in the measured NH_3 flux is the potential bias due to NH_4^+ deposition. As previously discussed, the chemiluminescence NH_3 analyzer used in this study detects an unknown fraction of NH_4^+ aerosol present in the sample. Based on long-term denuder/filter pack concentration measurements from a nearby site located at Clinton, NC (Walker et al., 2004), the ratio of NH_4^+ to NH_3 is 0.21 during the summer. Therefore, NH_3 concentrations measured with the chemiluminescence system may have been overestimated by 21% on average, assuming NH_4^+ was detected with 100% efficiency. Data from the Clinton site also show that NH_4^+ does not display a diurnal cycle, thus the chemiluminescence NH_3 concentration bias is smallest at night when NH_3 concentrations are higher ($\text{NH}_3/\text{NH}_4^+ = 0.16$) and largest during the day with NH_3 concentrations reach a minimum ($\text{NH}_3/\text{NH}_4^+ = 0.30$).

Assuming that the deposition flux measured with the chemiluminescence system represents total NH_x ($\text{NH}_x = \text{NH}_3 + \text{NH}_4^+$), the influence of NH_4^+ deposition on the measured NH_3 deposition velocity (i.e., the difference between measured and actual NH_3 deposition velocities) can be estimated from:

$$V_{\text{dNH}_3(\text{measured})} = \frac{\text{NH}_3}{\text{NH}_x} V_{\text{dNH}_3(\text{actual})} + \frac{\text{NH}_4^+}{\text{NH}_x} V_{\text{dNH}_4^+} \quad (13)$$

where the concentration ratios NH_3/NH_x and $\text{NH}_4^+/\text{NH}_x$ represent constants derived from the Clinton data set. For this analysis, the NH_4^+ deposition velocity was estimated using a modified version of Slinn's model (Ruijgrok et al., 1997). Following this approach, mean day and nighttime NH_3 deposition velocities (Table 3) may have been underestimated by 19% (19%) and 13% (12%), respectively, during dry (wet) periods. This

simple analysis, assuming a worst case scenario in which all of the NH_4^+ was measured as NH_3 , indicates that NH_4^+ deposition had a relatively minor effect on the measured NH_3 fluxes and deposition velocities. Differences in actual and measured NH_3 deposition velocities translate to overestimates in R_c of 35% (37%) and 22% (26%) during dry (wet) day and night periods, respectively. While NH_4^+ deposition does not fully explain the relatively high NH_3 canopy resistances observed at our site, the effect becomes more significant as $\text{NH}_3/\text{NH}_4^+$ decreases during the day.

While we have attempted to characterize the major sources of uncertainty in our measurements, our assessment is not comprehensive. For example, flux divergence due to chemical reactions is not quantified (Nemitz et al., 2004). Also, while our analysis focuses on average errors, it is likely that flux uncertainty displayed a diurnal cycle. Eddy diffusivities for sensible heat calculated using the Bowen-ratio approach are most uncertain in the early morning and late evening when the vertical temperature gradient is weak and the sensible heat flux becomes small. Also, uncertainty in the measured NH_3 gradient was largest in the morning when the ambient concentration was changing most rapidly (Fig. 2).

5. Conclusions

In general, the net deposition flux measured during this study was lower than expected. Our initial hypothesis was that the relatively high atmospheric NH_3 concentrations in our study area would correspond to high deposition rates. However, a number of factors may have contributed to the relatively low net deposition observed. First, high daytime temperatures resulted in a high average stomatal compensation point ($\approx 11.5 \mu\text{g NH}_3 \text{ m}^{-3}$). Modeling results suggest that uptake via the leaf cuticle was the dominant deposition process and stomatal uptake only occurred during the first few hours after sunrise when the stomatal resistance and compensation point were still low. Second, the measured cuticular resistance was large, most likely due to dry conditions and accumulation of NH_3 on leaf surfaces. The period of stomatal uptake in the morning may have increased the nitrogen status of the vegetation, thereby increasing the leaf emission potential. Our results are consistent with previous observations of low deposition rates to fertilized systems.

While the total amount of rainfall during the measurement period was typical of the summer period, the frequency of events was low. This led to extremely

dry conditions and the canopy often displayed visible signs of drought stress. Since it is evident that the NH_3 flux was affected by canopy dryness, it remains uncertain whether our results are representative of soybean within the study area. Also unclear is the extent to which drought stress may have influenced leaf apoplast chemistry and, therefore, the leaf NH_3 emission potential. While the results from this study are useful for determining overall deposition rates for the measurement period, additional measurements under conditions of adequate soil moisture are necessary to determine the extent to which plant moisture status may have influenced the process-level results reported in this paper.

Acknowledgements

We appreciate the technical support of Wayne Fowler, Chris Pressley, Mark Barnes, Jerome Miller, and Guillermo Ramirez throughout the course of the project. We also thank the two anonymous reviewers for their helpful comments and suggestions. Mention of trade names or commercial products does not constitute endorsement or recommendation of a commercial product. This research was funded by the U.S. Environmental Protection Agency, National Risk Management Research Laboratory, Research Triangle Park, NC.

References

- Adams, P.J., Seinfeld, J.H., Kotch, D.M., 1999. Global concentrations of tropospheric sulfate, nitrate, and ammonium aerosols simulated in a general circulation model. *J. Geophys. Res.* 104, 13791–13823.
- Aneja, V.P., Chauhan, J.P., Walker, J.T., 2000. Characterization of atmospheric ammonia emissions from swine waste storage and treatment lagoons. *J. Geophys. Res.* 105, 11535–11545.
- Ayers, G.P., 2001. Comment on regression analysis of air quality data. *Atmos. Environ.* 35, 2423–2425.
- Bouwman, A.F., Lee, D.S., Asman, W.A.H., Dentener, F.J., van der Hoek, K.W., Olivier, J.G.J., 1997. A global high-resolution emission inventory for ammonia. *Global Biogeochem. Cycles* 11, 561–587.
- Brady, N.C., Weil, R.R., 1999. *Elements of Nature and Properties of Soils*. Prentiss-Hall Inc., Upper Saddle River, NJ, 559 pp.
- Dabney, S.M., Bouldin, D.R., 1990. Apparent deposition velocity and compensation point of ammonia inferred from gradient measurements above and through alfalfa. *Atmos. Environ.* 24A, 2655–2666.
- Denmead, O.T., Nulsen, T., Thurtell, G.W., 1978. Ammonia exchange over a corn crop. *Soil Sci. Soc. Am. J.* 42, 840–842.
- Dentener, F.J., Crutzen, P.J., 1994. A three dimensional model for the global ammonia cycle. *J. Atmos. Chem.* 19, 331–369.
- Duyzer, J.H., Verhagen, H.L.M., Weststrate, J.H., 1992. Measurement of the dry deposition flux of NH_3 on to coniferous forest. *Environ. Pollut.* 75, 3–13.
- Duyzer, J., 1994. Dry deposition of ammonia and ammonium aerosols over heathland. *J. Geophys. Res.* 99, 18757–18763.
- Duyzer, J.H., Verhagen, H.L.M., Weststrate, J.H., Bosveld, F.C., Vermetten, A.W.M., 1994. The dry deposition of ammonia onto a Douglas Fir forest in The Netherlands. *Atmos. Environ.* 28, 1241–1253.
- Erisman, J.W., Wyers, G.P., 1993. Continuous measurements of surface exchange of SO_2 and NH_3 – implications for their possible interaction in the deposition process. *Atmos. Environ.* 27, 1937–1949.
- Erisman, J.W., Vanelzakker, B.G., Mennen, M.G., Hogenkamp, J., Zwart, E., Vandenbeld, L., Romer, F.G., Bobbink, R., Heil, G., Raessen, M., Duyzer, J.H., Verhage, H., Wyers, G.P., Otjes, R.P., Mols, J.J., 1994. The Elspeetsche Veld experiment on surface exchange of trace gases – summary of results. *Atmos. Environ.* 28, 487–496.
- Erisman, J.W., Grennfelt, P., Sutton, M., 2003. The European perspective on nitrogen emission and deposition. *Environ. Pollut.* 29, 311–325.
- Farquhar, G.D., Firth, P.M., Wetselaar, R., Weir, B., 1980. On the gaseous exchange of ammonia between leaves and the environment: determination of the ammonia compensation point. *Plant Physiol.* 66, 710–714.
- Finkelstein, P.L., Sims, P.F., 2001. Sampling error in eddy correlation flux measurements. *J. Geophys. Res.* 106, 3503–3509.
- Flechard, C.R., Fowler, D., 1998. Atmospheric ammonia at a moorland site. II: Longterm surface-atmospheric micrometeorological flux measurements. *Q. J. R. Met. Soc.* 124, 759–791.
- Flechard, C.R., Fowler, D., Sutton, M.A., Cape, J.N., 1999. A dynamic model of bi-directional ammonia exchange between semi-natural vegetation and the atmosphere. *Q. J. R. Meteorol. Soc.* 125, 2611–2641.
- Fowler, D., Unsworth, M.H., 1979. Turbulent transfer of sulphur dioxide to a wheat crop. *Q. J. R. Meteorol. Soc.* 105, 767–783.
- Fowler, D., Duyzer, J.H., 1989. Micrometeorological techniques for the measurement of trace gas exchange. In: Andreae, M.O., Schimel, D.S. (Eds.), *Exchange of Trace Gases between Terrestrial Ecosystems and the Atmosphere*. John Wiley and Sons Ltd., NJ, USA.
- Fowler, D., Pitcairn, C.E.R., Sutton, M.A., Flechard, C., Loubet, B., Coyle, M., Munro, R.C., 1998. The mass budget of atmospheric ammonia in woodland within 1 km of livestock buildings. *Environ. Pollut.* 102, 342–348.
- Garland, J.A., 1977. The dry deposition of SO_2 on agricultural crops. *Atmos. Environ.* 12, 369–373.
- Harper, L.A., Sharpe, R.R., Langdale, G.W., Giddens, J.E., 1987. Nitrogen cycling in a wheat crop: soil, plant, and aerial nitrogen transport. *Agron. J.* 79, 965–973.
- Harper, L.A., Sharpe, R.R., 1995. Nitrogen dynamics in irrigated corn: soil–plant nitrogen and atmospheric ammonia transport. *Agron. J.* 87, 669–675.
- Harper, L.A., Bussink, D.W., van der Meer, H.G., Corre, W.J., 1996. Ammonia transport in a temperate grassland. I. Seasonal transport in relation to soil fertility and crop management. *Agron. J.* 88, 614–621.
- Harper, L.A., Denmead, O.T., Sharpe, R.R., 2000. Identifying sources and sinks of scalars in a corn canopy with inverse Lagrangian dispersion analysis: II. Ammonia. *Agric. Forest Meteorol.* 104, 75–83.

- Hicks, B.B., Wesely, M.L., 1978. An examination of Some Micro-meteorological Methods for Measuring Dry Deposition. U.S. EPA Report, EPA-600/7-78-116. Research Triangle Park, North Carolina.
- Hicks, B.B., Baldocchi, D.D., Meyers, T.P., Hosker Jr., R.P., Matt, D.R., 1987. A preliminary multiple resistance routine for describing dry deposition velocities from measured quantities. *Water Air Soil Pollut.* 36, 311–330.
- Hsieh, C., Katul, G., Chi, T., 2000. An approximate analytical model for footprint estimation of scalar fluxes in thermally stratified atmospheric flows. *Adv. Water Resour.* 23, 765–772.
- Husted, S., Schjoerring, J.K., 1995. Apoplastic pH and ammonium concentration in leaves of *Brassica napus* L. *Plant Physiol.* 109, 1453–1460.
- Husted, S., Schjoerring, J.K., Nielson, K.H., Nemitz, E., Sutton, M., 2000. Stomatal compensation points for ammonia in oilseed rape plants under field conditions. *Agric. Forest Meteorol.* 105, 371–383.
- Israel, D.W., Burton, J.W., 1997. Nitrogen nutrition of soybean grown in Coastal Plain soils of North Carolina. Technical Bulletin 310, North Carolina Agricultural Service, North Carolina State University.
- Langford, A.O., Fehsenfeld, F.C., Zachariassen, J., Schimel, D.S., 1992. Gaseous ammonia fluxes and background concentrations in terrestrial ecosystems of the United States. *Global Biogeochem. Cycles* 6, 459–483.
- Malm, W.C., Sisler, J.F., Huffman, D., Eldred, R.A., Cahill, T.S., 1994. Spatial and seasonal trends in particle concentration and optical extinction in the United States. *J. Geophys. Res.* 99, 1347–1370.
- Mathur, R., Dennis, R.L., 2003. Seasonal and annual modeling of reduced nitrogen compounds over the eastern United States: emissions, ambient levels, and deposition amounts. *J. Geophys. Res.* 108 (D15), 4481, doi:10.1029/2002JD002794.
- Mattsson, M., Schjoerring, J.K., 2002. Dynamic and steady-state responses of inorganic nitrogen pools and NH₃ exchanges in leaves of *Lolium perenne* and *Bromus erectus* to changes in root nitrogen supply. *Plant Physiol.* 128, 742–750.
- Meixner, F.X., Wyers, G.P., Neftel, A., 1996. Bi-directional exchange of ammonia over cereals. In: Borrell, P.M., Borrell, P., Kelly, K., Cavitas, T., Seiler, W. (Eds.), *Proceedings of Eurotrac*. Computer Mechanics Publications, Southampton, Garmisch – Partenkirchen, pp. 129–135.
- Meyers, T.P., Hall, M.E., Lindberg, S.E., Kim, K., 1996. Use of the modified Bowen-ratio technique to measure fluxes of trace gases. *Atmos. Environ.* 30, 3321–3329.
- Meyers, T.P., Finkelstein, P.L., Clarke, J., Ellestad, T.G., Sims, P., 1998. A multilayer model for inferring dry deposition using standard meteorological measurements. *J. Geophys. Res.* 103, 22645–22661.
- Milford, C., Hargreaves, K.J., Sutton, M.A., Loubet, B., Cellier, P., 2001. Fluxes of NH₃ and CO₂ over upland moorland in the vicinity of agricultural land. *J. Geophys. Res.* 106 (D20), 24169–24181.
- Monteith, J.L., Unsworth, M., 1990. *Principles of Environmental Physics*, second ed. Arnold Press, London, 221 pp.
- NADP, 2004. National Atmospheric Deposition Program (NRSP-3). NADP Program Office, Illinois State Water Survey, Champaign, IL. <http://nadp.sws.uiuc.edu>.
- Nemitz, E., Sutton, M.A., Schjoerring, J.K., Husted, S., Wyers, G.P., 2000a. Resistance modeling of ammonia exchange over oilseed rape. *Agric. Forest Meteorol.* 105, 405–425.
- Nemitz, E., Sutton, M.A., Gut, A., San Jose, R., Husted, S., Schjoerring, J.K., 2000b. Sources and sinks of ammonia within an oilseed rape canopy. *Agric. Forest Meteorol.* 105, 385–404.
- Nemitz, E., Milford, C., Sutton, M.A., 2001. A two-layer canopy compensation point model for describing bi-directional biosphere-atmosphere exchange of ammonia. *Q. J. R. Meteorol. Soc.* 127, 815–833.
- Nemitz, E., Sutton, M.A., Wyers, G.P., Otjes, R.P., Mennen, M.G., van Putten, E.M., Gallagher, M.W., 2004. Gas–particle interactions above a Dutch heathland: II. Concentrations and surface exchange fluxes of atmospheric particles. *Atmos. Chem. Phys.* 4, 1007–1024.
- Nihlgard, B., 1985. The ammonium hypothesis – an additional explanation to the forest dieback in Europe. *Ambio* 14, 2–8.
- Paerl, H.W., 1995. Coastal eutrophication in relation to atmospheric nitrogen deposition: current perspectives. *Ophelia* 41, 237–259.
- Paerl, H.W., Whitall, D.R., 1999. Anthropogenically-derived atmospheric nitrogen deposition, marine eutrophication and harmful algal bloom expansion: is there a link? *Ambio* 28, 307–311.
- Phillips, S.B., Arya, S.P., Aneja, V.P., 2004. Ammonia flux and dry deposition velocity from near-surface concentration gradient measurements over a grass surface in North Carolina. *Atmos. Environ.* 38, 3469–3480.
- Pryor, S.C., Barthelmie, R.J., Sorenson, L.L., Jensen, B., 2001. Ammonia concentrations and fluxes over a forest in the midwestern USA. *Atmos. Environ.* 35, 5645–5656.
- Ratray, G., Sievering, H., 2001. Dry deposition of ammonia, nitric acid, ammonium, and nitrate to alpine tundra at Niwot Ridge, Colorado. *Atmos. Environ.* 35, 1105–1109.
- Robarge, W.P., Walker, J.T., McCulloch, R.B., Murray, G., 2002. Atmospheric concentrations of ammonia and ammonium at an agricultural site in the southeast United States. *Atmos. Environ.* 36, 1661–1674.
- Roelofs, J.G.M., Kempers, A.J., Houdijk, A.L.F.M., Jansen, J., 1985. The effect of airborne ammonium sulphate on *Pinus nigra* var. *maritima* in the The Netherlands. *Plant Soil* 84, 45–56.
- Ruijgrok, W., Tieben, H., Eisinga, P., 1997. The dry deposition of particles to a forest canopy: a comparison of model and experimental results. *Atmos. Environ.* 31, 399–415.
- Schjoerring, J.K., Husted, S., Mattsson, M., 1998. Physiological parameters controlling plant-atmosphere ammonia exchange. *Atmos. Environ.* 32, 491–498.
- Spindler, G., Teichmann, U., Sutton, M.A., 2001. Ammonia dry deposition over grassland – micrometeorological flux-gradient measurements and bidirectional flux calculations using an inferential model. *Q. J. R. Meteorol. Soc.* 127, 795–814.
- Sutton, M.A., Fowler, D., 1992. Dry deposition of ammonia to frozen land surfaces and analysis of the uncertainties in fluxes deriving from measurement errors. In: *Development of analytical techniques for atmospheric measurements*. Pap. COST 611 Workshop, CEC, Brussels, Rome, April.
- Sutton, M.A., Fowler, D., 1993. A model for inferring bi-directional fluxes of ammonia over plant canopies. In: *WMO Conference on the Measurement and Modeling of Atmospheric Composition Changes including Pollution Transport*, WMO/GAW, WMO, Geneva, CH, Sofia, Bulgaria, October, pp. 179–182.
- Sutton, M.A., Fowler, D., Moncrieff, J.B., Storeton-West, R.L., 1993a. The exchange of atmospheric ammonia with vegetated surfaces. II: Fertilized vegetation. *Q. J. R. Meteorol. Soc.* 119, 1047–1070.
- Sutton, M.A., Fowler, D., Moncrieff, J.B., 1993b. The exchange of atmospheric ammonia with vegetated surfaces. I: Unfertilized vegetation. *Q. J. R. Meteorol. Soc.* 119, 1023–1045.

- Sutton, M.A., Burkhardt, J.K., Guerin, D., Fowler, D., 1995. Measurements and modeling of ammonia exchange over arable croplands. In: Heij, G.J., Erisman, J.W. (Eds.), *Acid Rain Research: Do We Have Enough Answers*. Elsevier Science, BV.
- Sutton, M.A., Milford, C., Dragosits, U., Singles, R., Fowler, D., Ross, C., Hill, R., Jarvis, S.C., Pain, B.P., Harrison, R., Moss, D., Webb, J., Espenhahn, S.E., Halliwell, C., Lee, D.S., Wyers, G.P., Hill, J., ApSimon, H.M., 1997. Gradients of atmospheric ammonia concentrations and deposition downwind of ammonia emissions: first results of ADEPT Burrington Moore experiment. In: Jarvis, S.C., Payne, B.P. (Eds.), *Gaseous Exchange with Grassland Systems*. CAB International, Wallingford, Oxon, UK, pp. 131–139.
- Sutton, M.A., Burkhardt, J.K., Guerin, D., Nemitz, E., Fowler, D., 1998. Development of resistance models to describe measurements of bi-directional ammonia surface-atmosphere exchange. *Atmos. Environ.* 32, 473–480.
- Thompson, M., Howarth, R.J., 1976. Duplicate analysis in geochemical practice. Part I. Theoretical approach and estimation of analytical reproducibility. *Analyst* 101, 690–698.
- Tolocka, M.P., Solomon, P.A., Mitchell, W., Norris, G.A., Gemmill, D.B., Wiener, R.W., Vanderpool, R.W., Homolya, J.B., Rice, J., 2001. East versus west in the US: chemical characteristics of PM_{2.5} during the winter of 1999. *Aerosol. Sci. Technol.* 34, 8–96.
- USDA, 1954. Soil Survey of Duplin County, North Carolina. U.S. Department of Agriculture Natural Resources Conservation Service, Raleigh, North Carolina.
- U.S. EPA, 1997. National Ambient Air Quality Standards for Particulate Matter: Final Rule. Federal Register, vol. 62, no. 138.
- U.S. EPA, 1996. Air Quality Criteria for Particulate Matter. EPA/600/P-95/001aF. National Center for Environmental Assessment, Office of Research and Development, Research Triangle Park, NC.
- van Hove, L.W.A., Heeres, P., Bossen, M.E., 2002. The annual variation in stomatal ammonia compensation point of rye grass (*Lolium perenne* L.) leaves in an intensively managed grassland. *Atmos. Environ.* 36, 2965–2977.
- Walker, J.T., Aneja, V.P., Dickey, D., 2000a. Atmospheric transport and wet deposition of ammonium in North Carolina, USA. *Atmos. Environ.* 34, 3407–3418.
- Walker, J.T., Nelson, D., Aneja, V.P., 2000b. Trends in ammonium concentration in precipitation and atmospheric ammonia emissions at a Coastal Plain site in North Carolina, USA. *Environ. Sci. Technol.* 34, 3527–3534.
- Walker, J.T., Whittall, D., Robarge, W.P., Paerl, H., 2004. Ambient ammonia and ammonium aerosol across a region of variable ammonia emission density. *Atmos. Environ.* 38, 1235–1246.
- Weseley, M.L., 1989. Parameterization of surface resistances to gaseous dry deposition in regional-scale numerical models. *Atmos. Environ.* 23, 1293–1304.
- Yamulki, S., Harrison, R.M., Goulding, K.W.T., 1996. Ammonia surface exchange above an agricultural field in southeast England. *Atmos. Environ.* 30, 109–118.